

MPI-PhT/2002-56
KA-TP-16-2002
hep-ph/0210168

SIX-FERMION PRODUCTION AT e^+e^- COLLIDERS¹

STEFAN DITTMAYER¹ AND MARKUS ROTH²

¹ *Max-Planck-Institut für Physik (Werner-Heisenberg-Institut)*
D-80805 München, Germany

² *Institut für Theoretische Physik, Universität Karlsruhe*
D-76131 Karlsruhe, Germany

Abstract:

The class of six-fermion production processes at e^+e^- colliders comprises very interesting particle reactions, such as the production of top-quark pairs and of Higgs bosons in the intermediate Higgs mass range, the scattering of massive gauge bosons, and triple gauge-boson production. The Monte Carlo event generator LUSIFER is designed for the analysis of such processes. A few illustrating results obtained with LUSIFER are discussed.

October 2002

¹To appear in the proceedings of the *International Workshop on Linear Colliders*, August 26–30, 2002, Jeju Island, Korea.

SIX-FERMION PRODUCTION AT e^+e^- COLLIDERS

STEFAN DITTMAIER^{1†} and MARKUS ROTH²

¹ *Max-Planck-Institut für Physik (Werner-Heisenberg-Institut)
D-80805 München, Germany*

² *Institut für Theoretische Physik, Universität Karlsruhe
D-76131 Karlsruhe, Germany*

Abstract

The class of six-fermion production processes at e^+e^- colliders comprises very interesting particle reactions, such as the production of top-quark pairs and of Higgs bosons in the intermediate Higgs mass range, the scattering of massive gauge bosons, and triple gauge-boson production. The Monte Carlo event generator LUSIFER is designed for the analysis of such processes. A few illustrating results obtained with LUSIFER are discussed.

1 Introduction

The Monte Carlo event generator LUSIFER in its first version, which is described in Ref. [1] in detail, deals with all processes $e^+e^- \rightarrow 6$ fermions at tree level in the Standard Model. The predictions are based on the full set of Feynman diagrams, the number of which is typically of the order of 10^2 – 10^4 . Fermions other than top quarks, which are not allowed as external fermions, are taken to be massless, and polarization is fully supported. The helicity amplitudes are generically calculated with the spinor method of Ref. [2]. The phase-space integration is based on the

[†]e-mail address: dittmair@mppmu.mpg.de

multi-channel Monte Carlo integration technique [3], improved by adaptive weight optimization [4]. Channels and appropriate mappings are provided for each individual diagram in a generic way. More details on the phase-space parametrizations can be found in Refs. [5, 6]. Owing to the potentially large number of Feynman diagrams per final state, an efficient generic approach has been crucial, in order to gain an acceptable speed and stability of the program. Initial-state radiation is included at the leading logarithmic level employing the structure-function approach (see e.g. the appendix of Ref. [7]).

In the following we collect a few illustrating results of Ref. [1] that have been obtained with LUSIFER. In some cases, the tuned comparison with the combination of the WHIZARD [8] and MADGRAPH [9] packages is included in the discussion. Specifically, we focus on top-quark pair production, the production of Higgs bosons in the intermediate Higgs mass range, and the scattering of massive gauge bosons. The precise input for the used parameters and phase-space cuts, as well as much more results, can be found in Ref. [1]. We refer to the literature for further discussions of top-quark pair production [10, 11, 12], Higgs-boson production [12, 13], vector-boson scattering [14], and triple gauge-boson production [11, 12], which are also based on full $e^+e^- \rightarrow 6f$ matrix elements.

2 Results On Top-Quark Pair Production

In Table 1 we collect some results on cross sections that receive contributions from top-quark pair production, $e^+e^- \rightarrow t\bar{t} \rightarrow 6f$. The difference between the cross sections with two and four quarks in the final states roughly reflects the colour factor 3 between leptonically and hadronically decaying W bosons that have been produced in $t \rightarrow bW^+$. The cross sections are all strongly dominated by the signal diagrams for resonant $t\bar{t}$ production, which are identical for all considered final states. Differences are entirely due to so-called background diagrams, the size of which is, however, very sensitive to the angular separation cut between outgoing e^\pm and the beams. The inclusion of gluon-exchange diagrams would not influence the integrated cross section significantly. The numbers show that ISR reduces the cross sections at the level of $\sim 4\%$ at a centre-of mass (CM) energy of $\sqrt{s} = 500$ GeV. Finally, the comparison of the LUSIFER and WHIZARD & MADGRAPH results reveals good agreement.

3 Results On Higgs-Boson Production

In Figure 1 we show the invariant-mass (M_{4q}) and production angular (θ_{4q}) distributions for the four-quark system (including all $4q$ configurations of the first two generations) of the reactions $e^+e^- \rightarrow (\nu_\mu\bar{\nu}_\mu/\nu_e\bar{\nu}_e) + 4q$. The crucial difference between the $\nu_\mu\bar{\nu}_\mu$ and $\nu_e\bar{\nu}_e$ channels lies in the Higgs production mechanisms: while the former receives only contributions from ZH production, $e^+e^- \rightarrow Z + (H \rightarrow WW) \rightarrow 6f$, the latter additionally involves W fusion, $e^+e^- \rightarrow \nu_e\bar{\nu}_e + (WW \rightarrow H \rightarrow WW) \rightarrow 6f$, which dominates the cross section. Therefore, the cross section of $\nu_e\bar{\nu}_e + 4q$ is an order of magnitude larger than the one of $\nu_\mu\bar{\nu}_\mu + 4q$. The invariant-mass distributions of the two channels look similar, both showing the resonance peaks for the decays $H \rightarrow WW \rightarrow 4q$ at $M_{4q} = M_H$ which appear over a continuous background. Note that for $M_H = 190$ GeV and 230 GeV the high-energy tails of the distributions show some Higgs mass dependence. This is due to the subprocess of ZH production where the Higgs decays into on-shell Z bosons, $H \rightarrow ZZ \rightarrow (\nu_\mu\bar{\nu}_\mu/\nu_e\bar{\nu}_e) + 2q$, which is not yet possible for the smaller Higgs mass $M_H = 170$ GeV. The corresponding boundary in M_{4q} , which is clearly seen in the plots for $M_H = 190$ GeV, is determined by the two extreme situations where the decay $H \rightarrow ZZ$ proceeds along the ZH production axis. For $M_H = 230$ GeV this boundary is hidden by the Higgs peak and the upper kinematical limit in the M_{4q} spectrum. In contrast to the invariant-mass distributions, the shapes of the $4q$ angular distributions of the $\nu_\mu\bar{\nu}_\mu$ and $\nu_e\bar{\nu}_e$ channels look very different. For $\nu_\mu\bar{\nu}_\mu$, i.e. for ZH production, intermediate production angles dominate, and this dominance is more pronounced for smaller Higgs-boson masses, where more phase space is available. For $\nu_e\bar{\nu}_e$, i.e. W-boson fusion, forward

$e^+e^- \rightarrow$	LUSIFER		WHIZARD & MADGRAPH	
	$\sigma_{\text{Born}}[\text{fb}]$	$\sigma_{\text{Born+ISR}}[\text{fb}]$	$\sigma_{\text{Born}}[\text{fb}]$	$\sigma_{\text{Born+ISR}}[\text{fb}]$
$\mu^- \bar{\nu}_\mu \nu_\mu \mu^+ \text{bb}$	5.8091(49)	5.5887(36)	5.8102(26)	5.5978(30)
$\mu^- \bar{\nu}_\mu \nu_\tau \tau^+ \text{bb}$	5.7998(36)	5.5840(40)	5.7962(26)	5.5893(29)
$e^- \bar{\nu}_e \nu_\mu \mu^+ \text{bb}$	5.8188(45)	5.6042(38)	5.8266(27)	5.6071(30)
$e^- \bar{\nu}_e \nu_e e^+ \text{bb}$	5.8530(68)	5.6465(70)	5.8751(30)	5.6508(36)
$\mu^- \bar{\nu}_\mu \text{udbb}$	17.095(11)	16.4538(98)	17.1025(80)	16.4627(87)
$e^- \bar{\nu}_e \text{udbb}$	17.187(21)	16.511(12)	17.1480(82)	16.5288(92)

Table 1: Cross sections (without gluon-exchange diagrams) for top-quark pair production at $\sqrt{s} = 500$ GeV

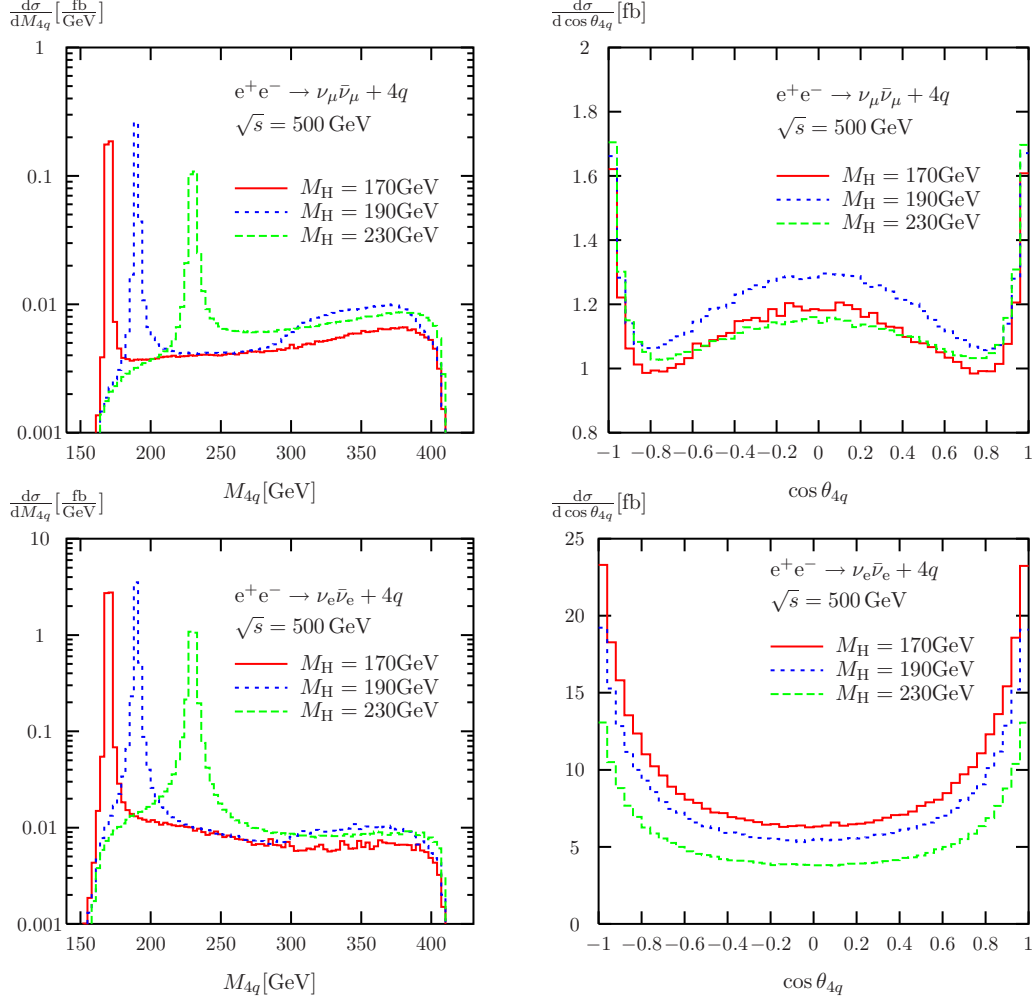


Figure 1: Invariant-mass and angular distributions of the $4q$ system in $e^+e^- \rightarrow (\nu_\mu \bar{\nu}_\mu / \nu_e \bar{\nu}_e) + 4q$ (without ISR and gluon-exchange diagrams) for various Higgs masses

$\sqrt{s} [\text{GeV}]$	500	800	1000	2000	10000
fixed width	1.6326(12)	4.1046(35)	5.6795(61)	11.736(16)	26.380(55)
running width	1.6398(12)	4.1324(39)	5.7206(54)	12.881(14)	12965(12)
complex mass	1.6330(12)	4.1037(34)	5.6705(54)	11.730(14)	26.387(57)

Table 2: Born cross sections in fb (without ISR) for $e^+e^- \rightarrow \nu_e \bar{\nu}_e \mu^- \bar{\nu}_\mu \text{ud}$ for various CM energies and schemes for introducing decay widths

and backward production of Higgs bosons is preferred, and the M_H dependence is mainly visible in the overall scale of the distribution, but not in the shape itself.

4 Results On Vector-Boson Scattering

Finally, in Table 2 we consider the high-energy behaviour of a typical channel involving the subprocess $WW \rightarrow WW$, using different schemes for introducing finite decay widths. This comparison is particularly important in order to control gauge-invariance violating effects in several schemes. In the *fixed-width scheme* all massive boson propagators receive a constant width Γ_B ($B = H, W, Z$), while in the *running width scheme* Γ_B is multiplied by $p^2/M_B^2 \times \theta(p^2)$, with p^2 denoting the virtuality of the propagator. Both schemes violate gauge invariance. In the *complex-mass scheme* [6], gauge invariance is restored by consistently using complex masses for the unstable particles in the Feynman rules, i.e. it makes use of the propagators of the fixed-width scheme and appropriately chosen complex couplings. The example confirms the expectation from $4f(+\gamma)$ studies [6] that the fixed-width scheme, in spite of violating gauge invariance, practically yields the same results as the complex-mass scheme. In contrast, the running-width scheme breaks gauge invariance so badly that deviations from the complex-mass scheme are already visible below 1 TeV. Above 1 TeV these deviations grow rapidly, and the high-energy limit of the prediction is totally wrong. Thus, if finite decay widths are introduced on cost of gauge invariance, the result is only reliable if it has been compared to a gauge-invariant calculation, as it is for instance provided by the complex-mass scheme. Moreover, our numerical studies (see also Ref. [1]) show that the fixed-width scheme is in fact a good candidate for reliable results also in six-fermion production, although it does not respect gauge invariance. Whether this observation generalizes to all $6f$ final states (or even further) is, however, not clear.

References

- [1] S. Dittmaier and M. Roth, Nucl. Phys. B **642** (2002) 307 [hep-ph/0206070].
- [2] S. Dittmaier, Phys. Rev. D **59** (1999) 016007 [hep-ph/9805445].

- [3] F. A. Berends, P. H. Daverveldt and R. Kleiss, Nucl. Phys. B **253** (1985) 441; J. Hilgart, R. Kleiss and F. Le Diberder, Comput. Phys. Commun. **75** (1993) 191.
- [4] R. Kleiss and R. Pittau, Comput. Phys. Commun. **83** (1994) 141 [hep-ph/9405257].
- [5] E. Byckling and K. Kajantie, “*Particle Kinematics*” (Wiley, London, 1973) p. 158ff; M. Roth, doctoral thesis, hep-ph/0008033.
- [6] A. Denner, S. Dittmaier, M. Roth and D. Wackerroth, Nucl. Phys. B **560** (1999) 33 [hep-ph/9904472].
- [7] W. Beenakker *et al.*, in *Physics at LEP2*, eds. G. Altarelli, T. Sjöstrand and F. Zwirner (CERN 96-01, Geneva, 1996), Vol. 1, p. 79 [hep-ph/9602351].
- [8] W. Kilian, LC-TOOL-2001-039, *2nd ECFA/DESY Study 1998-2001*, p. 1924.
- [9] T. Stelzer and W. F. Long, Comput. Phys. Commun. **81** (1994) 357 [hep-ph/9401258]; H. Murayama, I. Watanabe and K. Hagiwara, KEK-91-11.
- [10] F. Yuasa, Y. Kurihara and S. Kawabata, Phys. Lett. B **414** (1997) 178 [hep-ph/9706225]; F. Gangemi *et al.*, Nucl. Phys. B **559** (1999) 3 [hep-ph/9905271]; K. Kołodziej, Eur. Phys. J. C **23** (2002) 471 [hep-ph/0110063].
- [11] E. Accomando, A. Ballestrero and M. Pizzio, Nucl. Phys. B **512** (1998) 19 [hep-ph/9706201].
- [12] E. Accomando, A. Ballestrero and M. Pizzio, hep-ph/9709277.
- [13] G. Montagna, M. Moretti, O. Nicrosini and F. Piccinini, Eur. Phys. J. C **2** (1998) 483 [hep-ph/9705333]; E. Accomando, A. Ballestrero and M. Pizzio, Nucl. Phys. B **547** (1999) 81 [hep-ph/9807515]; F. Gangemi *et al.*, Eur. Phys. J. C **9** (1999) 31 [hep-ph/9811437].
- [14] F. Gangemi, hep-ph/0002142; R. Chierici, S. Rosati and M. Kobel, LC-PHSM-2001-038, *2nd ECFA/DESY Study 1998–2001*, p. 1906.